RESIDUAL STRESS ANALYSIS IN SEAMLESS API X60 STEEL GAS PIPELINES

Received 30/07/2002 – Accepted 09/03/2004

Abstract

This study is concerned with the analysis of residual strain and stress distributions through the wall of an API X60 grade high strength steel gas pipe. Residual stresses were measured using the BRSL method. This technique is based on the relaxation of stresses by splitting the tube in the longitudinal direction. Displacement measurements while notching indicated important shape changes before final split. Meanwhile, strain gages are used to monitor in real time strain behavior as a function of notch depth. It is found that relieved strains (μm/m) evolved from positive towards negative values in bored out and turned down cases. Circumferential residual stress distribution is obtained using both Mesnager-Sachs and Crampton equations. It is concluded that the latter gave realistic values as the distribution depicted compressive stresses on the outer layers and tensile stresses towards the pipe bore.

***Keywords**: Residual stress, Seamless steel pipeline, Pipe slitting, Layer removal.*

Résumé

Cette étude concerne l'analyse des déformations et des contraintes résiduelles à travers la paroi d'un tube de gaz en acier grade API X60 de haute résistance. Les contraintes résiduelles ont été mesurées par la méthode BRSL. Cette technique se base sur la relaxation des contraintes en sectionnant le tube dans la direction longitudinale. Les mesures de déplacement lors de la découpe ont montré d'importants changements dans la forme du tube avant rupture finale. En même temps, des jauges de déformation ont été utilisées pour enregistrer en temps réel le comportement de l'éprouvette en fonction de la profondeur de l'entaille. Pour les éprouvettes alésées ou chariotées, les déformations libérées (μm/m) évoluent de valeurs positives vers des valeurs négatives. Les contraintes résiduelles circonférentielles ont été obtenues en utilisant les deux équations proposées par Mesnager-Sachs et Crampton. Le modèle de Crampton donne des valeurs réalistes avec une distribution de contraintes allant de compressive sur les couches externes vers la traction dans les couches internes.

***Mots clés**: Contrainte résiduelle, Tube sans soudure, Découpe de tube, Enlèvement de couches.*

A. AMIRAT
K. CHAOUI
Laboratoire de Recherche Mécanique
des Matériaux et Maintenance Industrielle
(LR3MI)
Faculté des Sciences de l'Ingénieur
Département Génie Mécanique
Université Badji Mokhtar
BP 12, Annaba 23000, Algérie.

Z. AZARI
G. PLUVINAGE
Laboratoire de Fiabilité Mécanique
(LFM) Université de Metz
Ile du Saulcy
57045 Metz,Cedex 01, France.

ملخص

يهتم هذا البحث بدراسة توزيع التشوهات والاجهادات المتبقية عبر سمك قنوات الغاز الحديدية من فصيلة API X60. تم قياس الاجهادات المتبقية باستعمال طريقة BRSL (القطع والشق الطبقي بالجملة) التي تعتمد على استرخاء الاجهدات بالشق الطولي للقناة. سمحت هذا القيسات بالوقوف على تغيرات هامة في الشكل قبل القطع الكلي للأنبوب. تدل النتائج المحصلة عليها بأن التوزيع كان من قيم موجبة إلى قيم سالبة عند التنقل من السطح الخارجي نحو الداخل. و تم الحصول كذالك على توزيع الأجهدات المتبقية باستعمال قانوني Mesnager-Sachs وCrampton حيث أعطى هذا الأخير نتائج جد معقولة والتي أظهرت أن الأجهدات المتبقية كانت سالبة في الطبقات الخارجية وتتحول تدريجيا إلى موجبة في الطبقات الأخرى.

***الكلمات المفتاحية**: اجهدات متبقية، قناة غير ملحومة، شق القناة، نزع الطبقات.*

Seamless tubes made from high strength low alloy steel are usually used as basic structures to construct pipelines, often underground, for conveying pressurized gas over long distances. Consequently, gas pipelines are subjected to high stress and corrosive surroundings, which can lead to damage specifically under failed protective coating. The main causes of this damage are corrosion, stress corrosion cracking (SCC), fatigue crack propagation (FCP), wear, fouling and stress concentrators such as micro-cracks and inherent defects [1-6]. Therefore, research tendency is oriented to the improvement of material mechanical properties in terms of yield strength and toughness corrosion resistance [7-10]. Thermal and mechanical deformations, during the manufacturing process, always produce residual stresses. The generated stresses might be very high and sometimes approaching the material yield stress; however, their effects are not evident until the structure is loaded or exposed to an aggressive environment. It is agreed that tensile surface residual stresses are detrimental as they increase the susceptibility of components and structures to fatigue damage, stress corrosion and catastrophic failure. Usually, compressive surface residual stresses are beneficial, as they are deliberately introduced within the material using shot-peening or mechanical treatment techniques [11-13]. Nowadays, it is crucial that proper attention should be paid to estimating the magnitude and direction of the residual stresses in seamless tubes to assess correctly reliability estimates of tubular structures. The determination of through thickness

residual stress in pressure vessels is growing because of emphasis put on life prediction, design and failure analysis [4,8,14-16].

The purpose of the present study is to investigate residual strain evolution in high strength low alloy steel used to manufacture gas pipelines. Three aspects are considered: (a) shape changes due to notch depth progression, (b) strain relief behavior during notching and (c) residual stress distribution through pipeline wall. These results usually contribute to a better understanding of pipe life management and maintenance under service conditions.

1- THEORETICAL BACKGROUND

Residual stresses are those stresses locked into the material even when it is free from external forces. Fabricating processes, thermal processing, welding, heat treatment and mechanical forming are the most common sources of residual stresses. Practically, these stresses are present in every manufactured component and assembled structure. When producing tubes, residual stresses are generated from the hot rolling process that introduces large scale of deformations. The evaluation of the residual stresses can be carried out experimentally by means of destructive techniques known as Block Removal Splitting and Layering (BRSL) method based on the pioneering work developed by Sachs [17]. The Mesnager-Sachs method [18] consists of boring out the center of a cylinder in a succession of small layers and measuring changes in length and diameter of the remaining portion after each bore. Sachs proposed the following expressions for longitudinal, circumferential and radial stresses in hollow cylinders [17-19]:

$$\sigma_L = E'\left[\left(A_0 - A_b\right)\frac{d\lambda}{dA_b} - \lambda\right] \quad (1)$$

$$\sigma_c = E'\left[\left(A_0 - A_b\right)\frac{d\theta}{dA_b} - \frac{\theta(A_0 - A_b)}{2A_b}\right] \quad (2)$$

$$\sigma_r = E'\left[\frac{\theta\left(A_0 - A_b\right)}{2A_b}\right] \quad (3)$$

with: $$\lambda = \varepsilon_t + \nu\varepsilon_l \quad (4)$$

$$\theta = \varepsilon_l + \nu\varepsilon_t \quad (5)$$

and: $$E' = \frac{E}{1-\nu^2} \quad (6)$$

where E is the elastic modulus (MPa); A_0 is the original cross-sectional area of the cylinder; A_b is the area of the bored out portion of cylinder; (ε_l) and (ε_t) are longitudinal and circumferential strains respectively and ν is Poisson's ratio. This method is based on three basic assumptions: (a) elasticity theory equations apply for stresses in tubes subjected to internal or external pressures, (b) stress distribution is axi-symmetric and constant along tube length and (c) a material layer removal is accompanied by an equal and homogeneous change in longitudinal stress [17]. These assumptions are usually met without difficulties but the measuring and calculation processes are not evident. In a simpler approach, Crampton [19] has developed a measuring technique for circumferential residual stresses in thin tubing by slitting the entire length longitudinally and measuring diameter change. Hence, circumferential stress is expressed in terms of wall thickness (t), original (D_0) and final (D_1) diameters as follows:

$$\sigma_c = E't\left(\frac{1}{D_0} - \frac{1}{D_1}\right) \quad (7)$$

The tube length (L), according to the Crampton method, should obey the geometrical condition:

$$\frac{L}{D_0} \geq 2 \quad (8)$$

The effect of tube length on the results obtained by this method has been studied separately [20] and it was concluded that a ratio of 1.7 can be used adequately to meet the requirement of equation (8). Many other methods reviewed by J.R. Sorem *et al.* [21] have been developed to measure residual stresses in pipes for axial direction such as those used by Popelar *et al*. and Cheng *et al*. combining strain gages and axial slits. In the circumferential direction, experimental methods for determining non-axisymmetric through thickness residual stresses are limited to the original procedure developed by Rosenthal and Norton. Non-axisymmetric cases represent an important class of residual stress analysis problems including seam welded pipes and pressure vessels [22, 23].

2- EXPERIMENTAL DETAILS

2.1- Material

The examined work material is a normal API pipe steel of grade X60. It is typically used for the production of seamless tubes by hot rolling. The Algerian Steel Company, ALFATUB of Groupe SIDER at Annaba generously supplied the pipe portion. The chemical composition and mechanical properties are respectively given in Tables 1 and 2. The average external diameter and wall thickness were respectively 219 mm and 12.7 mm. The pipe material was not subjected to any other treatment after rolling operation.

Element	C	Mn	Si	S	Al
%	0.29-0.34	1.15-1.35	0.15-0.30	<0.025	<0.025
Element	Cr	Mo	Ti	V	
%	0.05-0.65	<0.05	<0.04	0.03-0.07	

Table 1: Chemical composition in weight % for X60 seamless tube steel.

Specimen Number	TT (°C)	$\sigma_{0.2}$ (MPa)	σ_u (MPa)	A (%)	Hardness (HV_{30})
1	200	1107	1477	13.3	474
2	300	1173	1385	13.5	438
3	400	1139	1257	14	399
4	500	1007	1080	16.5	354
5	600	779	865	20.5	281

Table 2: Effect of tempering temperature (TT) on mechanical properties of X60 grade steel.

2.2- Specimen preparation

All specimens were machined from a parent pipe with a total length of 12000 mm. Specimen cuts were performed in the tube production workshop of ALFATUB Co. on a specially designed Bardons turning machine where the rotational movement is given to the whole tube and the feed rate to the cutting tool. The dimensions of each specimen were recorded and then, ten (10) specimens, each 450 mm long and weighting 47 kg, were prepared so as to have gradual thickness reduction from 12.7 to 2 mm. The layer removal operations were accomplished on a lathe in the metal cutting workshop of the Algerian FERROVIAL Co., by boring out. The cutting conditions were a speed of 10 m/min, a feed rate of 0.10 mm/rev and a cut depth of 0.25 mm. Since much care was necessary when manipulating heavy specimen and clamping it into the four jaws of lathe spindle, the machining process was time consuming. In addition, one tube was also turned down to a wall thickness of 3.5 mm. The thickness of each specimen was measured at 8 equidistant points by means of a precision micrometer and the external and internal diameters were recorded using vernier calipers.

2.3- Measurement techniques

In order to measure residual displacements and strains due to cutting process, the tube was mounted on a horizontal milling machine and clamped with a purpose designed device as to fix it at the lower point and open it on the opposite point as shown in figure 1.

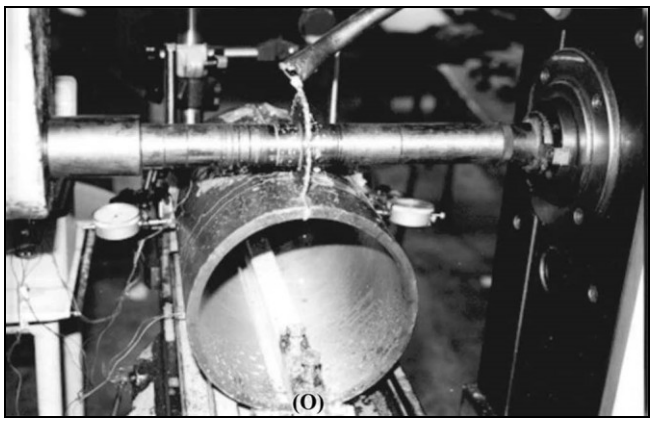

Figure 1: Photography of a tube specimen mounted on a horizontal milling machine and being cut longitudinally with a disk saw. Point (O) is constrained.

This apparatus allowed all other points of the tube to freely move in all directions, when a notch was introduced along specimen length. The notch was deepened progressively by means of a 2 mm thick disk mill; using controlled regular depth passes of 0.25 mm until the final cut. Each pass was followed by displacement and strain measurements. Displacement results were achieved by installing four precision dial indicators to record changes in diameter. The lower point, designated by (O) in Figure 1, was fixed and served as a clamping area. Indicators "1" and "2" measured the displacements perpendicular to the machined notch while indicators "3" and "4" were placed approximately 5 mm apart, symmetric to the notch. Figure 2a illustrates the tube as mounted on the machine and as instrumented for strain and displacement recordings. Relieved strains were obtained by bounding strain gauges (Type Micro-Measurements, EA-13-125AD-120) on the specimens. The layout is presented in figure 2b, with 3 pairs of strain gauges at an angle of 120° on the external surface and 2 pairs at 90° on the internal surface. The strain gauge readings were made on a 10 output Wheatstone bridge data logger.

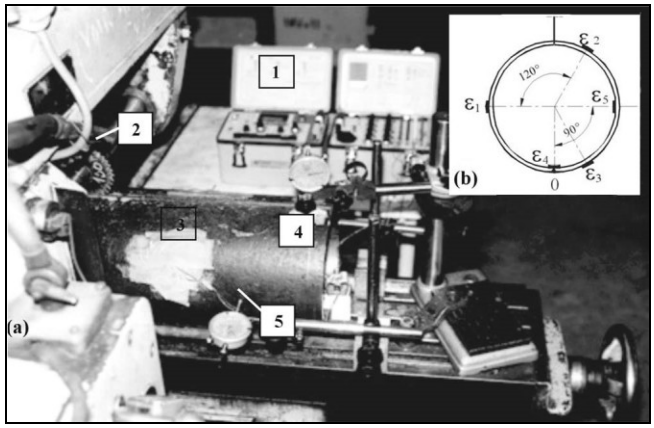

Figure 2: (a) General view of strain and displacement measurement layout; 1. Wheatstone bridge, 2. Disk mill, 3. Protected strain gauges, 4. Tube specimen, 5. Micrometer dial; **(b)** Strain gauge positions.

Because of its importance and dominance, circumferential residual stress distribution was determined using the layer removal method. Changes in diameter were recorded to allow the circumferential stress to be calculated from the relaxed strain after tube opening, according to equations (2) and (7). Figure 3 shows internal and external views of a tube after band saw opening. The corresponding calculated residual stresses were then plotted as a function of dimensionless wall thickness.

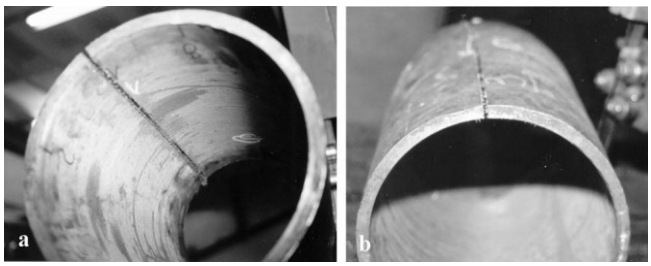

Figure 3: Internal **(a)** and external **(b)** views of a tube specimen after opening.

3- RESULTS AND DISCUSSION

3.1- Opening displacement

The first apparent effect of residual stresses was observed from the precision dial indicators. The evolution of residual displacements as a function of depth notch is illustrated in figures 4 and 5. In the as-received specimen, during notch progression, displacements Δ_1 and Δ_2 were negative and directed towards the center of the tube whilst

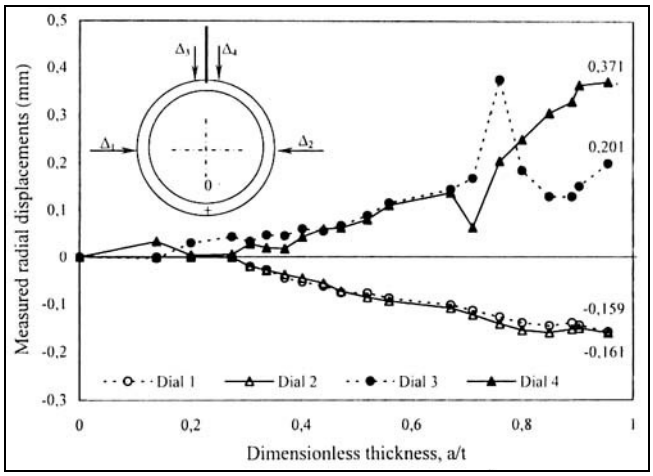

Figure 4: Evolution of measured radial displacements as a function of notch depth for the as-received tube (D_0=219.7 mm; t=12.7 mm; V12).

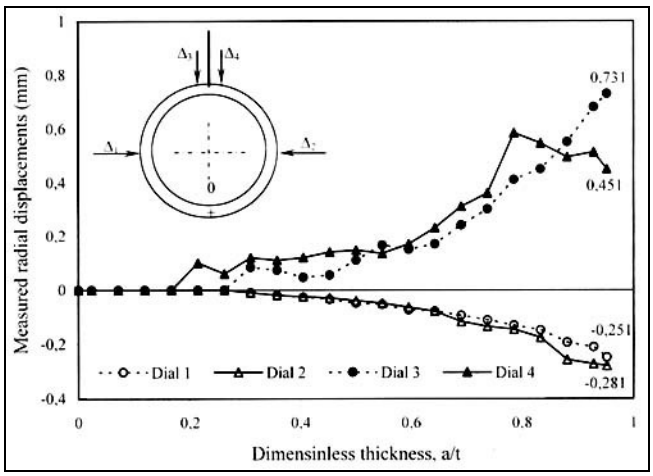

Figure 5: Evolution of measured radial displacements as a function of notch depth for the case of bored out tube to t=10.5 mm (V2).

displacements Δ_3 and Δ_4 moved towards the outside, away from the center, resulting in an oval form. These changes in specimen geometry were followed with crack opening displacements (COD) which were difficult to measure and are not reported here. When the final thin layer (0.25 mm thick) was cut, the tube popped up suddenly and was accompanied with a sound wave sometimes well before reaching specimen mid-length. This situation resulted in a jump up of displacement values as indicated in table 3, allowing the tube to be in a continual search of intermediate forms to accommodate relieved strains until final shape. This means that the center point of the opened tube can be derived from the mean differences of measured displacements. In this case, the center point was shifted to 2.2 mm and 1.38 mm according to *X* and *Y* axes respectively. Similar observations were made when the tube was bored out to 10.5 mm thickness as shown in Figure 5. However, displacements were almost two folds than those obtained in the as-received specimen. After opening, the final displacements were not significantly different as depicted in Table 3 indicating an equilibrium state for a cylindrical form. When observing thinner specimen, as in the case of turned down tube to 3.5 mm thickness, the measurements were too difficult to carry out. In fact, when reducing wall thickness, the tube became less rigid and the influence of applied cutting force caused high deformations and important vibrations to occur. The use of strain gauges was then of great help in following residual strains.

	D_0=219.7; t=12.7mm		D_0=219.7; t=10.5mm	
Dial	Δ_{j-1} (mm)	Δ_j (mm)	Δ_{j-1} (mm)	Δ_j (mm)
1	- 0.16	1.82	- 0.25	2.10
2	- 0.16	2.27	- 0.23	2.30
3	0.37	1.40	0.47	1.70
4	0.20	1.93	0.45	1.83

Table 3: Residual displacements before and after tube opening.
Δ_{j-1} : is the last recorded displacement before tube opening.
Δ_j : is the final displacement after tube opening.

Specimen Number	D_0 (mm)	D_1 (mm)	Thickness range (mm)	δ_c[a] (mm)	δ_L[b] (mm)	Observation
V11	217.80	200.90	1.80 to 2.40	-30.6	5.0	bored out, closing
V10	218.65	214.40	2.90 to 3.05	-15.0	1.0	bored out, closing
V3	218.45	218.20	4.90 to 5.50	-3.0	<1.0	bored out, closing
V7	218.60	217.80	5.35 to 6.20	-2.8	<0.5	bored out, closing
V6	218.55	218.20	6.40 to 7.25	-2.4	-	bored out, closing
V5	218.90	219.20	7.55 to 8.40	+0.3	-	bored out, opening
V4	218.70	219.00	8.25 to 9.95	+0.4	-	bored out, opening
V8	218.85	219.60	9.65 to 10.35	+1.8	-	bored out, opening
V2	218.50	219.00	9.95 to 11.25	+1.25	1.5	bored out, opening
V12	219.10	221.00	12.20 to 13.30	+0.7	<1.0	as-received, opening
V13[c]	199.40	200.00	2.50 to 4.40	+0.2	<1.0	turned down, opening

Table 4: Dimensional measurement results after tube slitting. [a]: Circumferential displacement; [b]: Longitudinal displacement; [c]: Turned down tube from 219.7 to 199.4 mm.

When varying the thickness (*t*) by boring out, the tube closed as the wall is thinned down from 12.7 mm to 2 mm and allowed a longitudinal displacement (δ_L) to take place as shown in table 4. In fact, specimens V5, V4, V8, V2 and V12 exhibited an opening final displacement (δ_c) ranging between +0.3 to +1.8mm. On the other part, V11, V10, V3, V7 and V6 handed up with overlapping displacements in the interval of -2.4 to -30.6mm. Some of the slit specimens and the corresponding average thickness $< t_i >$ are presented in figure 6.

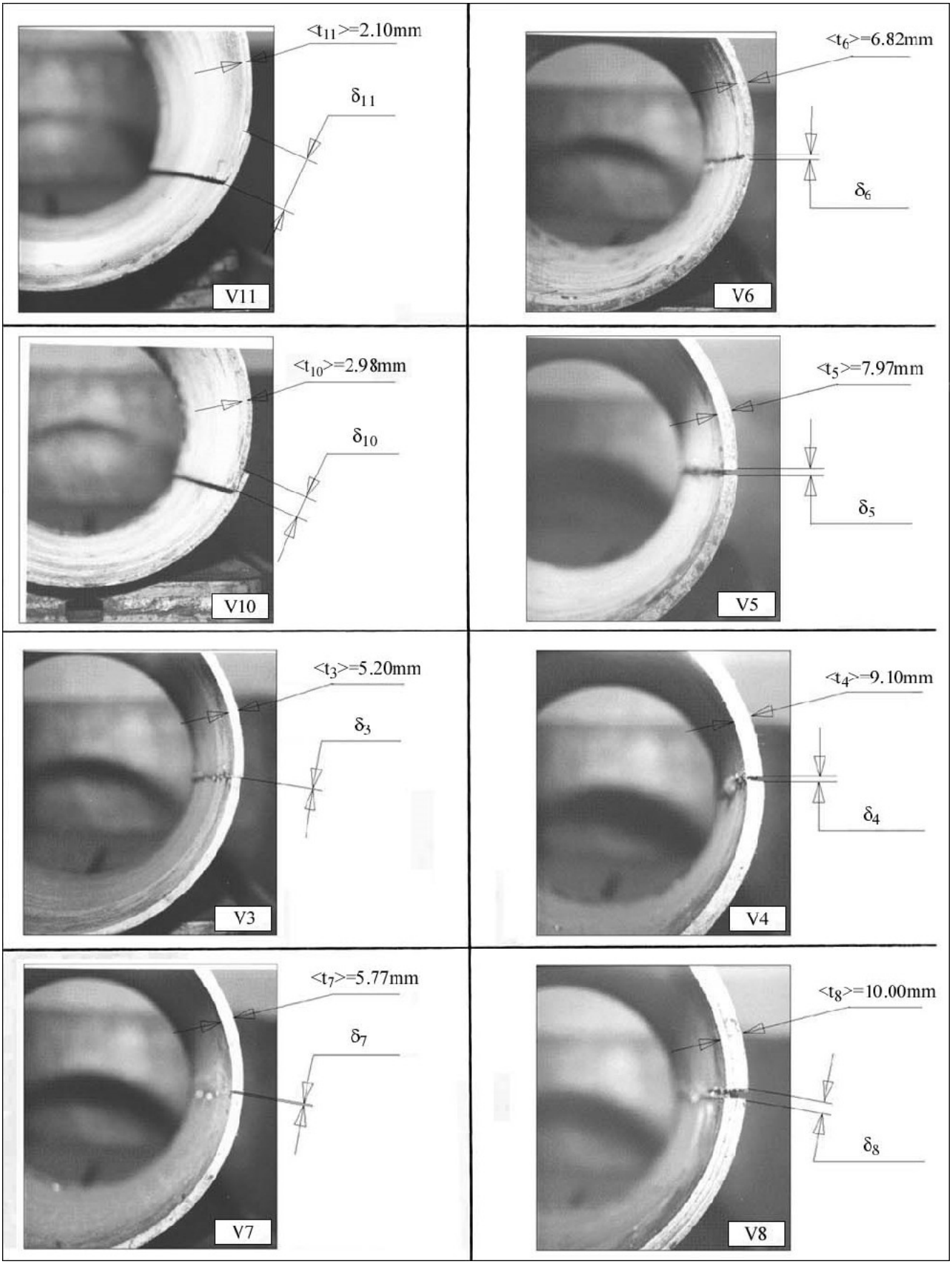

Figure 6: Behavior of bored out tube after slitting at various mean thickness, $\langle t_i \rangle$. The obtained displacement is represented by δ_i .

The removal of compressive layers produced strain relaxation within the tensile layers in order to conserve an equilibrium state imposed by the residual stress redistribution. The behavior of circumferential displacements after tube slitting is presented in figure 7 as a function of the remaining mean wall thickness. The data obeyed a logarithmic law, with a high correlation coefficient, in the form:

$$\delta_c = 16.38 Ln\, t - 35.48 \qquad (9)$$

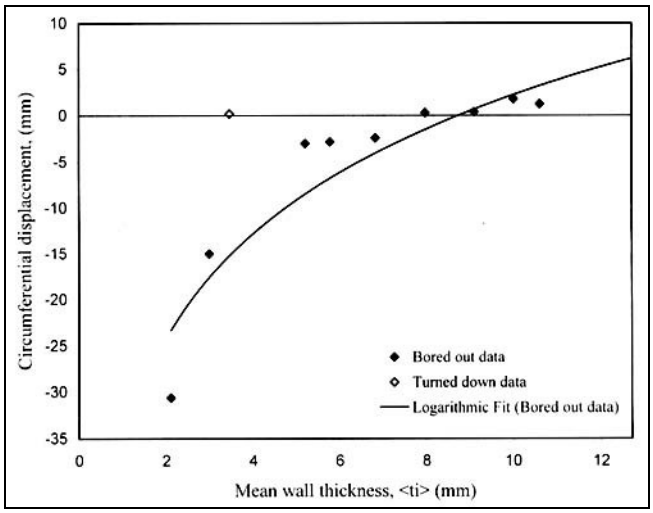

Figure 7: Circumferential displacement after tube slitting as a function of remaining mean wall thickness.

Basically, over-lapping was important compared to opening as the production process deformed plastically the external layers of the obtained cylinder by continuous metal rolling at high temperature and high surface pressures. Removal of 65% of wall thickness caused large scales of compression that resulted in specimen closure. Compared to a wall thickness of 10 mm, the closure displacement was 17 times higher than that of 2 mm which exhibited the highest longitudinal displacement (Table 4). In the same order of idea, specimen V13 was turned down to 3.5 mm to examine the expected final opening as compared to V11. It was found that the ratio rose even higher to 153 times.

3.2- Depth effect on residual strain

The strain gauge measurements revealed the behavior of the residual strains while notching progression. This is illustrated in figures 8, 9 and 10. For the as-received specimen, the relieved strain evolutions of ε_1 and ε_3 showed practically similar trends, with a gap of approximately 130 µm/m. In addition, ε_2 was negligible since it was placed near the cutting area. For specimen V2 that is thick and bored out, similar behavior was observed but the relieved strains were almost 4 folds as they reached a maximum of 590 µm/m. For the turned down specimen and before final opening, the strains were even higher as deformations were facilitated because of the lower overall stiffness. In every case, ε_3 and ε_4 showed opposite signs as expected from the initial gauge locations. The behavior of ε_4 for the 3 cases (V2, V12 and V13) is plotted in figure 11.

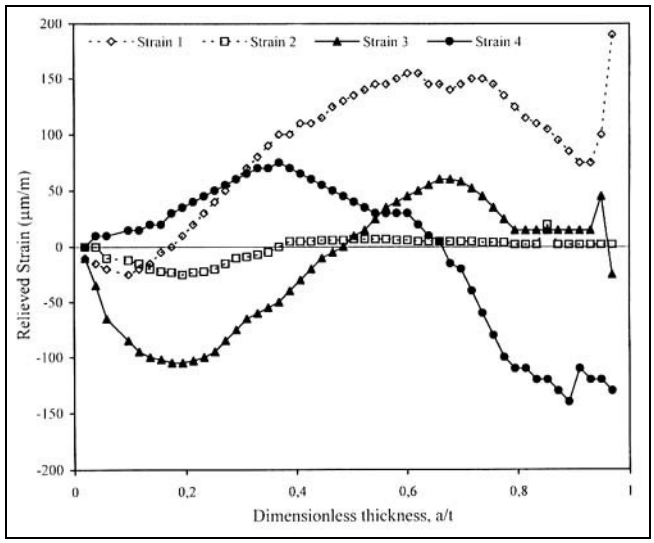

Figure 8: Relieved strain behavior as a function of longitudinal notch depth in the as-received tube, specimen V12 (measuring step 0.5 mm).

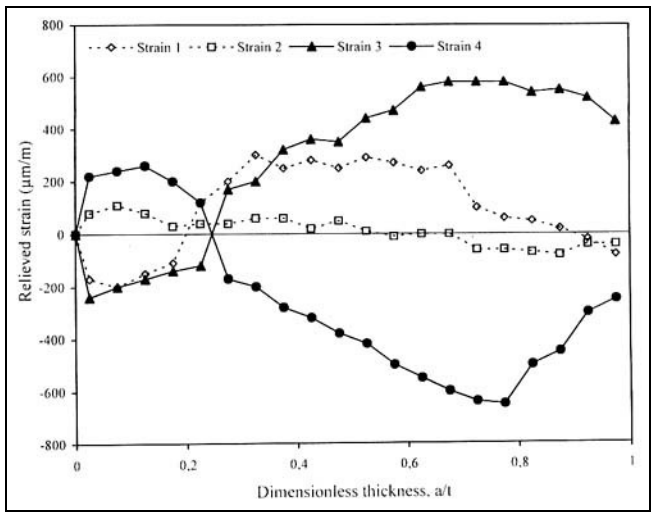

Figure 9: Relieved strain behavior as a function of longitudinal notch depth in bored out tube, specimen V2 (measuring step 1 mm).

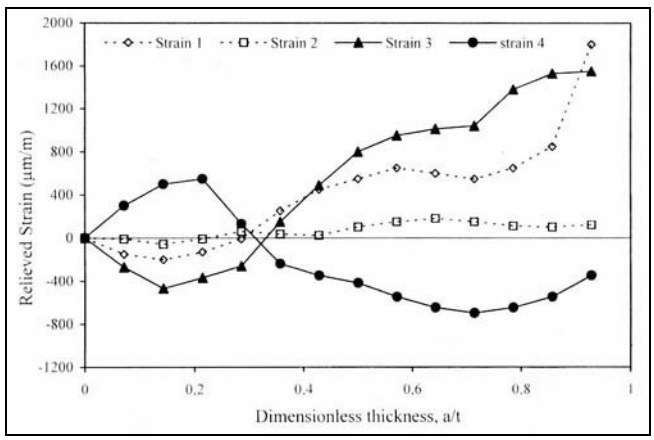

Figure 10: Relieved strain behavior as a function of longitudinal notch depth in turned down tube, specimen V13 (measuring step 1 mm).

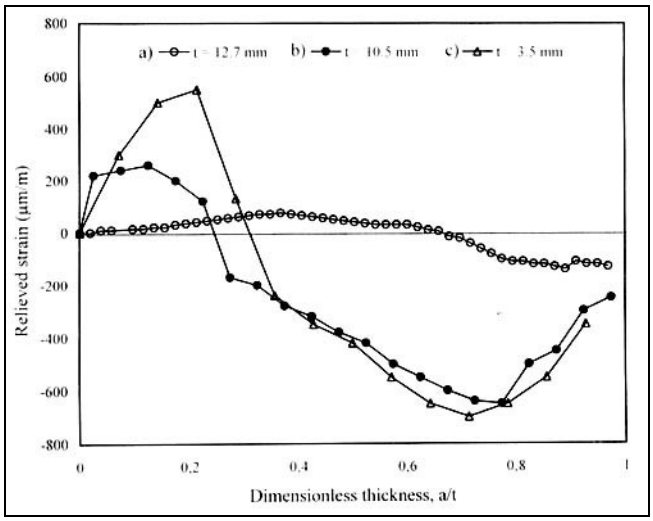

Figure 11: Comparison between relieved strains obtained by gauge 4, in the a) as-received, b) bored out and c) turned down specimens.

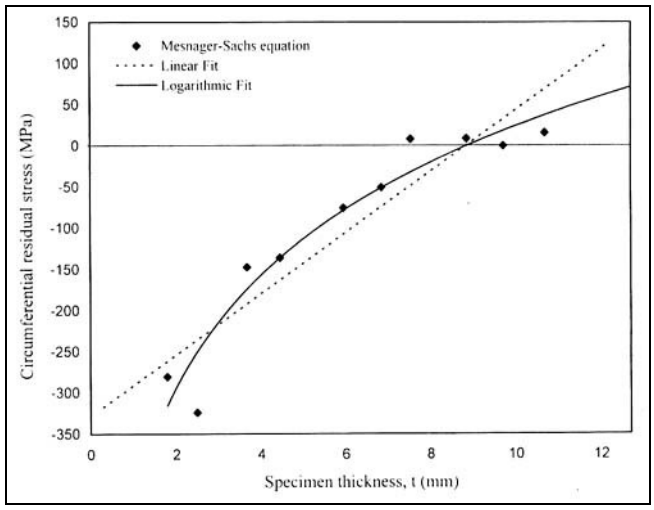

Figure 12: Circumferential residual stress distribution according to Mesnager-Sachs equation.

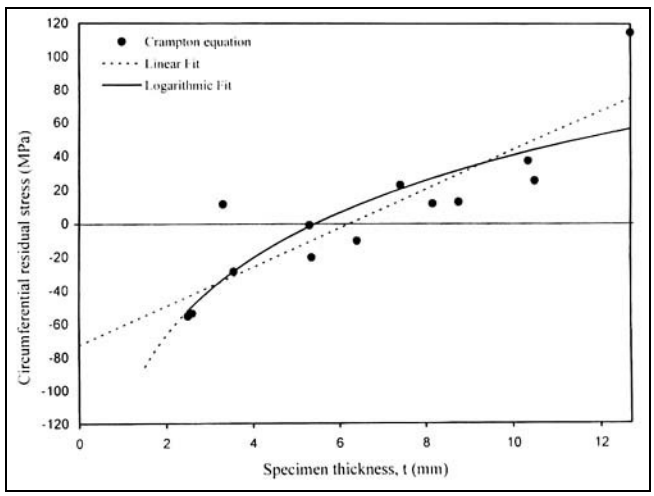

Figure 13: Circumferential residual stress distribution according to Crampton equation.

It is observed that the curves exhibited the same trend especially for V2 and V13. For a t=3.5 mm, ε_4 rose up to +550 μm/m and went down to -700 μm/m when the as-received fluctuated between +75 and -140 μm/m. A net difference was obtained when comparing zero relieved strain values.

3.3- Residual stress distribution

Using equations (2) and (7), circumferential residual stress distributions through wall thickness were obtained as illustrated respectively in figures 12 and 13. As tube thickness was reduced by layer removal from the inner side, the value of the residual stress decreased and changed sign from positive to negative. This finding confirmed that of displacements in figure 7. The calculated values presented some dispersion which was attributed to machining processes and to pipe inherent heterogeneity due to rolling. These results are comparable to those of literature [11-13,21-25] for piping and welding. The Mesnager-Sachs distribution (Fig. 12) was considered to be less effective since it does not account for the effect of longitudinal strains and gave high compressive stresses with a skewed distribution. Alternatively, the proposed equation by Crampton represented in a better way the distribution. This is obvious for the linear fit which generated an equilibrated distribution. Both data were subjected to logarithmic fits and the results are as follows:

Mesnager-Sachs equation:

$$\sigma_c = 206.13 Lnt - 482.66 \quad (10)$$

Crampton equation:

$$\sigma_c = 124.02 Lnt - 239.04 \quad (11)$$

The correlation coefficients were respectively 0.93 and 0.86. It is important to note that the zero value was approximately at 7.6 mm from the external diameter for the second case. The residual stresses at the pipe outer surface and at the bore were in the interval -156.3 MPa and +101.3 MPa that represented approximately 10 % of the material yield strength [20, 26]. These results may be used to study the effect of residual stress on reliability of underground pipes subjected to uniform corrosion and stress corrosion cracking phenomena.

CONCLUSION

The distribution of residual stresses through wall tube thickness was obtained by the layer removal method. It was found that compressive stresses acted on the outside layers of the pipe while tensile values dominated the bore side. The zero stress value was found at 7.6 mm depth using the Crampton equation, which exhibited a more realistic distribution, compared to Mesnager-Sachs model. This behavior is in good agreement with strain measurements during the cutting process. As the cutting notch was deepened, negative strain values are recorded passing by a zero value at 6.1 mm depth to become positive strains. The maximum residual stress value represented 10% of the material yield strength, a value that is fairly high to participate in damage due to stress corrosion cracking.

***Acknowledgments*:** We are grateful to ALFATUB Company for the furniture of the material and mechanical testing. We are also thankful to FERROVIAL Company for machining the large and heavy specimens. The financial support of SONATRACH National Oil Company, DP, Hassi Messaoud under Grant D-6001Z is greatly appreciated.

REFERENCES

[1]- Parkins R.N., Fesler R.R., "Line pipe stress corrosion cracking mechanisms and remedies", *Corrosion*, Paper N° 320 (1986).

[2]- Shahinian P., Judy R.W. Jr., "Stress corrosion crack growth in surface cracked panels of high strength steels", Stress corrosion - New approaches, ASTM, STP 610 (1976), pp.128-142.

[3]- Gray J.M., Pontremoly M., "Metallurgical options for grades X70 and X80 line pipe", International Conference on Pipe Technology, Rome, (1987), pp.171-191.

[4]- Shi P., Mahadevan S., "Corrosion fatigue and multiple site damage reliability analysis", *Int. J. Fatigue*, Vol. 25 (2003), pp.457-469.

[5]- Moulin D., Clement G., Drubay B., Goudet G., "Evaluation of ductile tearing in cracked pipes and elbows under bending", Nuclear Engineering and Design, Vol. 171 (2003), pp.33-43.

[6]- Orynyak I.V., Torop V.M., "Modelling of the limit state of thin-walled pipes with multiple axial coplanar defects", *Int. J. Pres. Ves. & Piping*, Vol. 70 (1996), pp.111-115.

[7]- Endos S. Nagae M., "Development of X100 UOE line pipe", The International Conference on Pipe Line Reliability, Calgary, 3 (1992), pp. 4.1-4.11.

[8]- Chattopadhyay J. Dutta, B.K., Kushwaha, H.S., Mahajan S.C., Kadodkar A., "Limit load analysis and safety assessment of an elbow with a circumferential crack under a bending moment", *Int. J. Pres. Ves. & Piping*, Vol. 62 (1995), pp.100-116.

[9]- Firmature R., Rahman S., "Elastic-plastic analysis of off-center cracks in cylindrical structures", *Engineering Fracture Mechanics*, Vol. 66 (2000), pp.15-39.

[10]- Michel B., Plancq D., "Lower bound limit load of a circumferentially cracked pipe under combined mechanical loading", *Nuclear Engineering and Design*, Vol. 185 (1998), pp.23-31.

[11]- Prevéy P.S., Cammett J.T., "The effect of shot-peening coverage on residual stress, cold work and fatigue in Ni-Cr-Mo low alloy steel", Proceedings of The International Conference on Shot-Peening, Sept. 16-20, Garmisch-Partenkirchen, Germany, (2002).

[12]- Prevéy P. Hornbach D. Mason P. Mahoney M., "Improving corrosion fatigue performance of AA2219 friction stir welds with low plasticity burnishing", International Surface Engineering Conference, Oct. 7-10, Columbus, OH. (2002).

[13]- Prevéy P., Hornbach D., Mason P., "Thermal residual stress relaxation and distortion in surface enhanced gas turbine engine components", Proceedings of the 17th Heat Treating Society Conference and Exposition, Eds. D.L. Milam et al., ASM, Materials Park, OH. (1998), pp.3-12.

[14]- Ahammed M., Melchers R.E., "Reliability estimation of pressurized pipelines subject to localized corrosion defects", *Int. J. Pres. Ves. & Piping*, Vol. 69 (1996), pp.267-272.

[15]- Kim Y.J, Schwalbe K.–H, Ainsworth R.A., "Simplified J-estimations based on the engineering treatment model for homogeneous and mismatched structures", *Engineering Fracture Mechanics,* Vol. 68 (2001), pp.9-27.

[16]- Zerbst U., Ainsworth R.A., Schwalbe K.-H., "Basic principles of analytical flaw assessment methods", *Int. J. Pres. Ves. & Piping*, Vol.77 (2000), pp.855-867.

[17]- Sachs G., "Internal stresses in metals", Zeitschrift des Vereines Deutcher Ingenieure, 71 (1927), pp.1511-1516.

[18]- Barrett C.S., "Internal stresses-A review", Metals and Alloys, 5 (1934), pp.131-154.

[19]- Lynch J.J., "The measurement of residual stresses", American Society for Metals, Residual Stress Measurements, Cleveland, OH. (1952), pp. 42-96.

[20]- Amirat A, Chaoui K., "Residual stress in seamless tubes", Synthèse, Revue des Sciences et Technologies de l'Université d'Annaba, (2001), pp.82-86.

[21]- Sorem Jr. J.R, Shadley J.R, Rybicki E.F., "Experimental method for determining through thickness residual hoop stresses in thin walled pipes and tubes without inside access", *Strain*, Vol. 26 (1990), pp.7-14.

[22]- Glinka G., "Residual stresses in fatigue and fracture: Theoretical analyses and experiments", in Residual stresses–generation, relaxation, measurement, prediction effects. A. Niku-Lari, Editor, Pergamon Press Ltd., UK (1986).

[23]- Ueda Y., Nakacho K., Shimizu T., "Improvement of residual stresses of circumferential joint of pipe by heat-sink welding", *Transactions of the ASME*, 108 (1986), pp.14-23.

[24]- ASTM STP 676, "Stress relaxation testing", Fox A., Editor, Philadelphia, PA., Committee E-28, (1979).

[25]- Harvey J.F., "Theory and Design of Pressure Vessels", Van Nostrand Reinhold Co. Inc., New York (1985).

[26]- Chaoui K., Amirat A., "Residual stress analysis in seamless X60 steel gas pipelines", 5ème Journées Scientifiques et Techniques, Hilton Hotel, Algiers, 16-18 December (2002)□

residual stress in pressure vessels is growing because of emphasis put on life prediction, design and failure analysis [4,8,14-16].

The purpose of the present study is to investigate residual strain evolution in high strength low alloy steel used to manufacture gas pipelines. Three aspects are considered: (a) shape changes due to notch depth progression, (b) strain relief behavior during notching and (c) residual stress distribution through pipeline wall. These results usually contribute to a better understanding of pipe life management and maintenance under service conditions.

1- THEORETICAL BACKGROUND

Residual stresses are those stresses locked into the material even when it is free from external forces. Fabricating processes, thermal processing, welding, heat treatment and mechanical forming are the most common sources of residual stresses. Practically, these stresses are present in every manufactured component and assembled structure. When producing tubes, residual stresses are generated from the hot rolling process that introduces large scale of deformations. The evaluation of the residual stresses can be carried out experimentally by means of destructive techniques known as Block Removal Splitting and Layering (BRSL) method based on the pioneering work developed by Sachs [17]. The Mesnager-Sachs method [18] consists of boring out the center of a cylinder in a succession of small layers and measuring changes in length and diameter of the remaining portion after each bore. Sachs proposed the following expressions for longitudinal, circumferential and radial stresses in hollow cylinders [17-19]:

$$\sigma_L = E'\left[\left(A_0 - A_b\right)\frac{d\lambda}{dA_b} - \lambda\right] \quad (1)$$

$$\sigma_c = E'\left[\left(A_0 - A_b\right)\frac{d\theta}{dA_b} - \frac{\theta(A_0 - A_b)}{2A_b}\right] \quad (2)$$

$$\sigma_r = E'\left[\frac{\theta\left(A_0 - A_b\right)}{2A_b}\right] \quad (3)$$

with: $$\lambda = \varepsilon_t + \nu\varepsilon_l \quad (4)$$

$$\theta = \varepsilon_l + \nu\varepsilon_t \quad (5)$$

and: $$E' = \frac{E}{1-\nu^2} \quad (6)$$

where E is the elastic modulus (MPa); A_0 is the original cross-sectional area of the cylinder; A_b is the area of the bored out portion of cylinder; (ε_l) and (ε_t) are longitudinal and circumferential strains respectively and ν is Poisson's ratio. This method is based on three basic assumptions: (a) elasticity theory equations apply for stresses in tubes subjected to internal or external pressures, (b) stress distribution is axi-symmetric and constant along tube length and (c) a material layer removal is accompanied by an equal and homogeneous change in longitudinal stress [17]. These assumptions are usually met without difficulties but the measuring and calculation processes are not evident. In a simpler approach, Crampton [19] has developed a measuring technique for circumferential residual stresses in thin tubing by slitting the entire length longitudinally and measuring diameter change. Hence, circumferential stress is expressed in terms of wall thickness (t), original (D_0) and final (D_1) diameters as follows:

$$\sigma_c = E't\left(\frac{1}{D_0} - \frac{1}{D_1}\right) \quad (7)$$

The tube length (L), according to the Crampton method, should obey the geometrical condition:

$$\frac{L}{D_0} \geq 2 \quad (8)$$

The effect of tube length on the results obtained by this method has been studied separately [20] and it was concluded that a ratio of 1.7 can be used adequately to meet the requirement of equation (8). Many other methods reviewed by J.R. Sorem *et al.* [21] have been developed to measure residual stresses in pipes for axial direction such as those used by Popelar *et al*. and Cheng *et al*. combining strain gages and axial slits. In the circumferential direction, experimental methods for determining non-axisymmetric through thickness residual stresses are limited to the original procedure developed by Rosenthal and Norton. Non-axisymmetric cases represent an important class of residual stress analysis problems including seam welded pipes and pressure vessels [22, 23].

2- EXPERIMENTAL DETAILS

2.1- Material

The examined work material is a normal API pipe steel of grade X60. It is typically used for the production of seamless tubes by hot rolling. The Algerian Steel Company, ALFATUB of Groupe SIDER at Annaba generously supplied the pipe portion. The chemical composition and mechanical properties are respectively given in Tables 1 and 2. The average external diameter and wall thickness were respectively 219 mm and 12.7 mm. The pipe material was not subjected to any other treatment after rolling operation.

Element	C	Mn	Si	S	Al
%	0.29-0.34	1.15-1.35	0.15-0.30	<0.025	<0.025
Element	Cr	Mo	Ti	V	
%	0.05-0.65	<0.05	<0.04	0.03-0.07	

Table 1: Chemical composition in weight % for X60 seamless tube steel.

Specimen Number	TT (°C)	$\sigma_{0.2}$ (MPa)	σ_u (MPa)	A (%)	Hardness (HV_{30})
1	200	1107	1477	13.3	474
2	300	1173	1385	13.5	438
3	400	1139	1257	14	399
4	500	1007	1080	16.5	354
5	600	779	865	20.5	281

Table 2: Effect of tempering temperature (TT) on mechanical properties of X60 grade steel.

2.2- Specimen preparation

All specimens were machined from a parent pipe with a total length of 12000 mm. Specimen cuts were performed in the tube production workshop of ALFATUB Co. on a specially designed Bardons turning machine where the rotational movement is given to the whole tube and the feed rate to the cutting tool. The dimensions of each specimen were recorded and then, ten (10) specimens, each 450 mm long and weighting 47 kg, were prepared so as to have gradual thickness reduction from 12.7 to 2 mm. The layer removal operations were accomplished on a lathe in the metal cutting workshop of the Algerian FERROVIAL Co., by boring out. The cutting conditions were a speed of 10 m/min, a feed rate of 0.10 mm/rev and a cut depth of 0.25 mm. Since much care was necessary when manipulating heavy specimen and clamping it into the four jaws of lathe spindle, the machining process was time consuming. In addition, one tube was also turned down to a wall thickness of 3.5 mm. The thickness of each specimen was measured at 8 equidistant points by means of a precision micrometer and the external and internal diameters were recorded using vernier calipers.

2.3- Measurement techniques

In order to measure residual displacements and strains due to cutting process, the tube was mounted on a horizontal milling machine and clamped with a purpose designed device as to fix it at the lower point and open it on the opposite point as shown in figure 1.

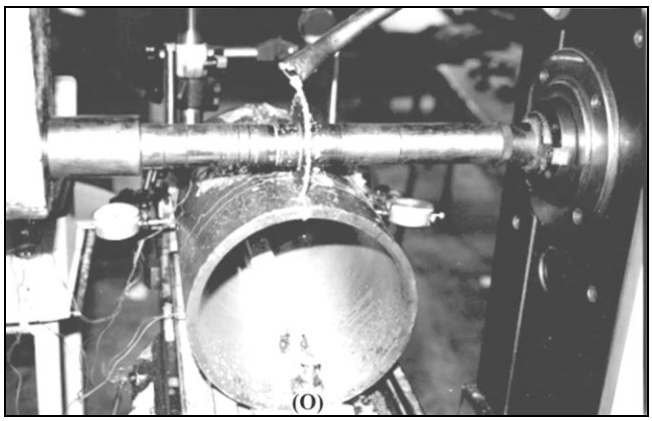

Figure 1: Photography of a tube specimen mounted on a horizontal milling machine and being cut longitudinally with a disk saw. Point (O) is constrained.

This apparatus allowed all other points of the tube to freely move in all directions, when a notch was introduced along specimen length. The notch was deepened progressively by means of a 2 mm thick disk mill; using controlled regular depth passes of 0.25 mm until the final cut. Each pass was followed by displacement and strain measurements. Displacement results were achieved by installing four precision dial indicators to record changes in diameter. The lower point, designated by (O) in Figure 1, was fixed and served as a clamping area. Indicators "1" and "2" measured the displacements perpendicular to the machined notch while indicators "3" and "4" were placed approximately 5 mm apart, symmetric to the notch. Figure 2a illustrates the tube as mounted on the machine and as instrumented for strain and displacement recordings. Relieved strains were obtained by bounding strain gauges (Type Micro-Measurements, EA-13-125AD-120) on the specimens. The layout is presented in figure 2b, with 3 pairs of strain gauges at an angle of 120° on the external surface and 2 pairs at 90° on the internal surface. The strain gauge readings were made on a 10 output Wheatstone bridge data logger.

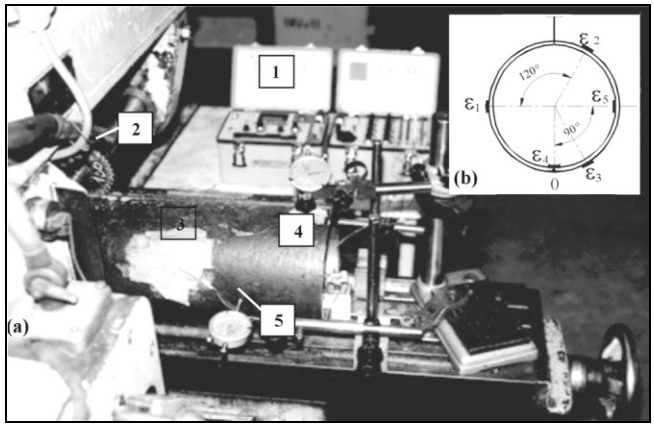

Figure 2: (a) General view of strain and displacement measurement layout; 1. Wheatstone bridge, 2. Disk mill, 3. Protected strain gauges, 4. Tube specimen, 5. Micrometer dial; **(b)** Strain gauge positions.

Because of its importance and dominance, circumferential residual stress distribution was determined using the layer removal method. Changes in diameter were recorded to allow the circumferential stress to be calculated from the relaxed strain after tube opening, according to equations (2) and (7). Figure 3 shows internal and external views of a tube after band saw opening. The corresponding calculated residual stresses were then plotted as a function of dimensionless wall thickness.

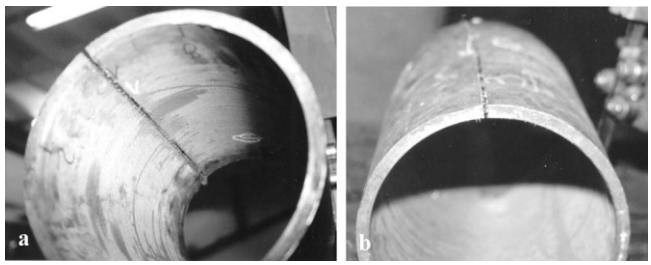

Figure 3: Internal **(a)** and external **(b)** views of a tube specimen after opening.

3- RESULTS AND DISCUSSION

3.1- Opening displacement

The first apparent effect of residual stresses was observed from the precision dial indicators. The evolution of residual displacements as a function of depth notch is illustrated in figures 4 and 5. In the as-received specimen, during notch progression, displacements Δ_1 and Δ_2 were negative and directed towards the center of the tube whilst

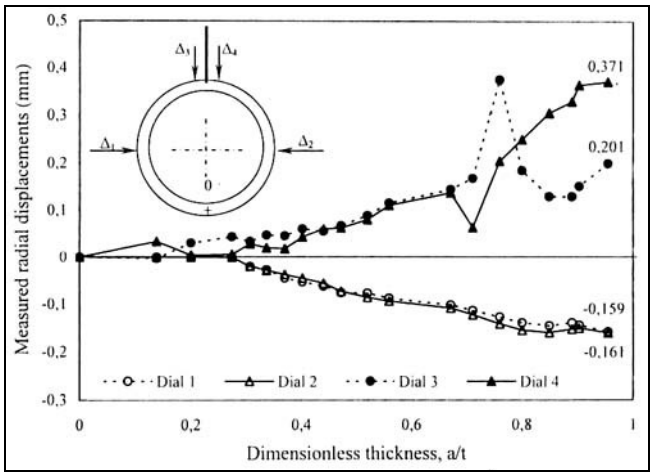

Figure 4: Evolution of measured radial displacements as a function of notch depth for the as-received tube (D_0=219.7 mm; t=12.7 mm; V12).

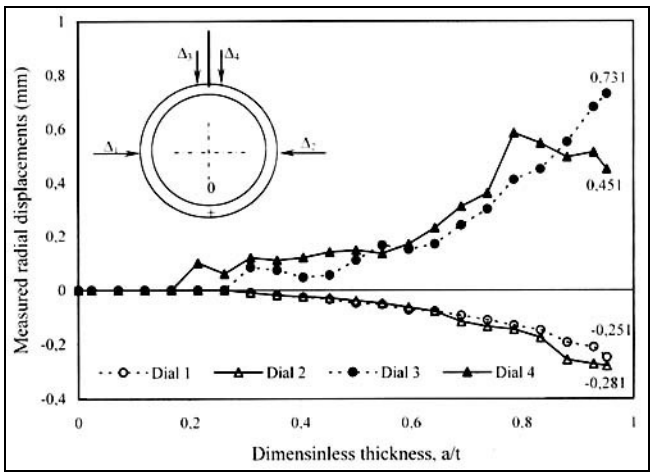

Figure 5: Evolution of measured radial displacements as a function of notch depth for the case of bored out tube to t=10.5 mm (V2).

displacements Δ_3 and Δ_4 moved towards the outside, away from the center, resulting in an oval form. These changes in specimen geometry were followed with crack opening displacements (COD) which were difficult to measure and are not reported here. When the final thin layer (0.25 mm thick) was cut, the tube popped up suddenly and was accompanied with a sound wave sometimes well before reaching specimen mid-length. This situation resulted in a jump up of displacement values as indicated in table 3, allowing the tube to be in a continual search of intermediate forms to accommodate relieved strains until final shape. This means that the center point of the opened tube can be derived from the mean differences of measured displacements. In this case, the center point was shifted to 2.2 mm and 1.38 mm according to *X* and *Y* axes respectively. Similar observations were made when the tube was bored out to 10.5 mm thickness as shown in Figure 5. However, displacements were almost two folds than those obtained in the as-received specimen. After opening, the final displacements were not significantly different as depicted in Table 3 indicating an equilibrium state for a cylindrical form. When observing thinner specimen, as in the case of turned down tube to 3.5 mm thickness, the measurements were too difficult to carry out. In fact, when reducing wall thickness, the tube became less rigid and the influence of applied cutting force caused high deformations and important vibrations to occur. The use of strain gauges was then of great help in following residual strains.

	D_0=219.7; t=12.7mm		D_0=219.7; t=10.5mm	
Dial	Δ_{j-1} (mm)	Δ_j (mm)	Δ_{j-1} (mm)	Δ_j (mm)
1	- 0.16	1.82	- 0.25	2.10
2	- 0.16	2.27	- 0.23	2.30
3	0.37	1.40	0.47	1.70
4	0.20	1.93	0.45	1.83

Table 3: Residual displacements before and after tube opening.
Δ_{j-1} : is the last recorded displacement before tube opening.
Δ_j : is the final displacement after tube opening.

Specimen Number	D_0 (mm)	D_1 (mm)	Thickness range (mm)	δ_c[a] (mm)	δ_L[b] (mm)	Observation
V11	217.80	200.90	1.80 to 2.40	-30.6	5.0	bored out, closing
V10	218.65	214.40	2.90 to 3.05	-15.0	1.0	bored out, closing
V3	218.45	218.20	4.90 to 5.50	-3.0	<1.0	bored out, closing
V7	218.60	217.80	5.35 to 6.20	-2.8	<0.5	bored out, closing
V6	218.55	218.20	6.40 to 7.25	-2.4	-	bored out, closing
V5	218.90	219.20	7.55 to 8.40	+0.3	-	bored out, opening
V4	218.70	219.00	8.25 to 9.95	+0.4	-	bored out, opening
V8	218.85	219.60	9.65 to 10.35	+1.8	-	bored out, opening
V2	218.50	219.00	9.95 to 11.25	+1.25	1.5	bored out, opening
V12	219.10	221.00	12.20 to 13.30	+0.7	<1.0	as-received, opening
V13[c]	199.40	200.00	2.50 to 4.40	+0.2	<1.0	turned down, opening

Table 4: Dimensional measurement results after tube slitting. [a]: Circumferential displacement; [b]: Longitudinal displacement; [c]: Turned down tube from 219.7 to 199.4 mm.

When varying the thickness (*t*) by boring out, the tube closed as the wall is thinned down from 12.7 mm to 2 mm and allowed a longitudinal displacement (δ_L) to take place as shown in table 4. In fact, specimens V5, V4, V8, V2 and V12 exhibited an opening final displacement (δ_c) ranging between +0.3 to +1.8mm. On the other part, V11, V10, V3, V7 and V6 handed up with overlapping displacements in the interval of -2.4 to -30.6mm. Some of the slit specimens and the corresponding average thickness $< t_i >$ are presented in figure 6.

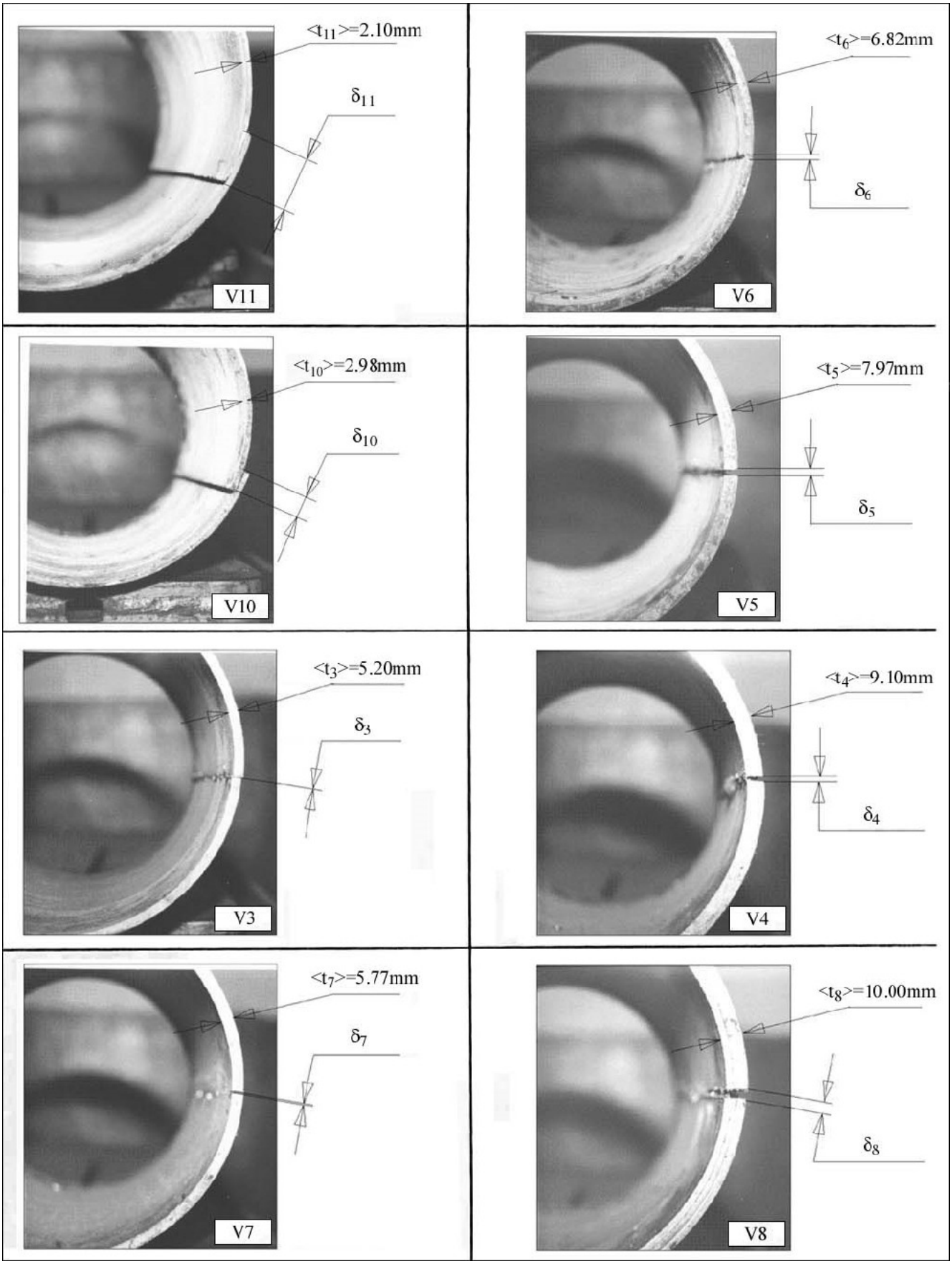

Figure 6: Behavior of bored out tube after slitting at various mean thickness, $\langle t_i \rangle$. The obtained displacement is represented by δ_i .

The removal of compressive layers produced strain relaxation within the tensile layers in order to conserve an equilibrium state imposed by the residual stress redistribution. The behavior of circumferential displacements after tube slitting is presented in figure 7 as a function of the remaining mean wall thickness. The data obeyed a logarithmic law, with a high correlation coefficient, in the form:

$$\delta_c = 16.38 Ln\, t - 35.48 \qquad (9)$$

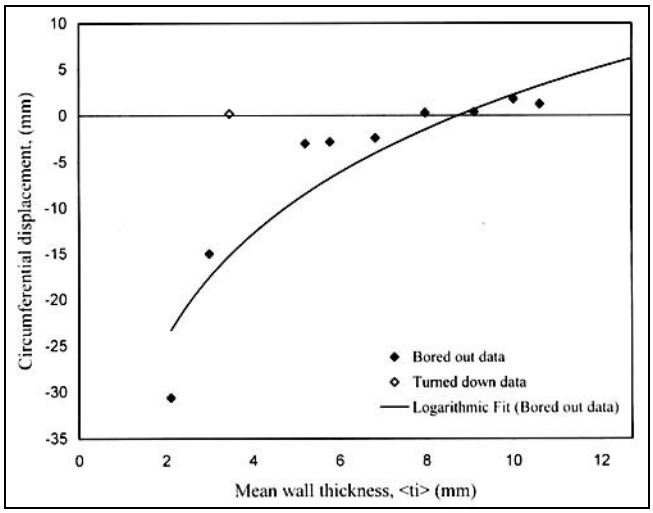

Figure 7: Circumferential displacement after tube slitting as a function of remaining mean wall thickness.

Basically, over-lapping was important compared to opening as the production process deformed plastically the external layers of the obtained cylinder by continuous metal rolling at high temperature and high surface pressures. Removal of 65% of wall thickness caused large scales of compression that resulted in specimen closure. Compared to a wall thickness of 10 mm, the closure displacement was 17 times higher than that of 2 mm which exhibited the highest longitudinal displacement (Table 4). In the same order of idea, specimen V13 was turned down to 3.5 mm to examine the expected final opening as compared to V11. It was found that the ratio rose even higher to 153 times.

3.2- Depth effect on residual strain

The strain gauge measurements revealed the behavior of the residual strains while notching progression. This is illustrated in figures 8, 9 and 10. For the as-received specimen, the relieved strain evolutions of ε_1 and ε_3 showed practically similar trends, with a gap of approximately 130 µm/m. In addition, ε_2 was negligible since it was placed near the cutting area. For specimen V2 that is thick and bored out, similar behavior was observed but the relieved strains were almost 4 folds as they reached a maximum of 590 µm/m. For the turned down specimen and before final opening, the strains were even higher as deformations were facilitated because of the lower overall stiffness. In every case, ε_3 and ε_4 showed opposite signs as expected from the initial gauge locations. The behavior of ε_4 for the 3 cases (V2, V12 and V13) is plotted in figure 11.

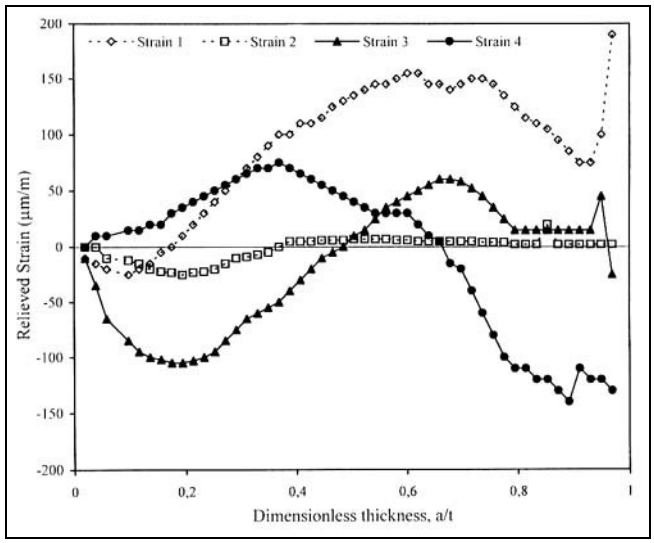

Figure 8: Relieved strain behavior as a function of longitudinal notch depth in the as-received tube, specimen V12 (measuring step 0.5 mm).

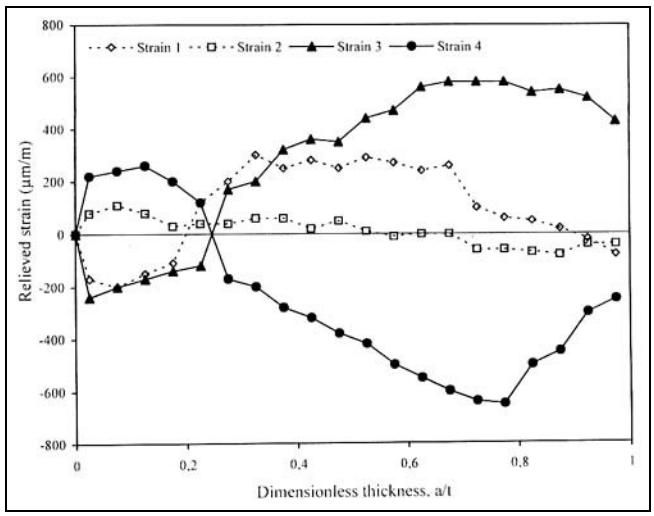

Figure 9: Relieved strain behavior as a function of longitudinal notch depth in bored out tube, specimen V2 (measuring step 1 mm).

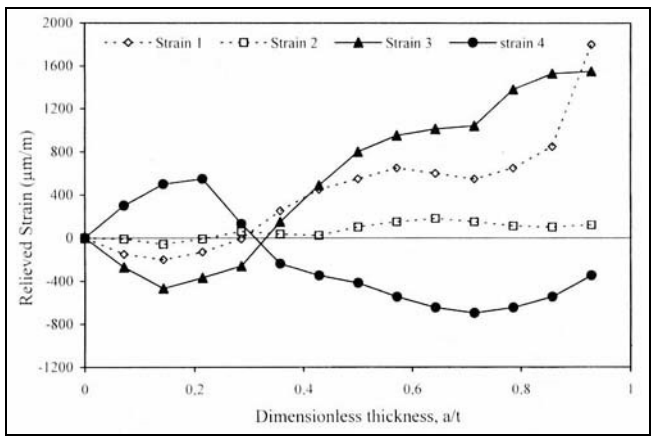

Figure 10: Relieved strain behavior as a function of longitudinal notch depth in turned down tube, specimen V13 (measuring step 1 mm).

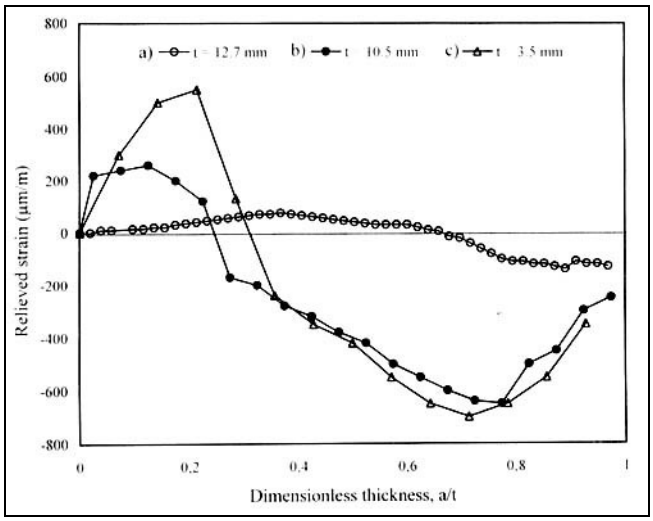

Figure 11: Comparison between relieved strains obtained by gauge 4, in the a) as-received, b) bored out and c) turned down specimens.

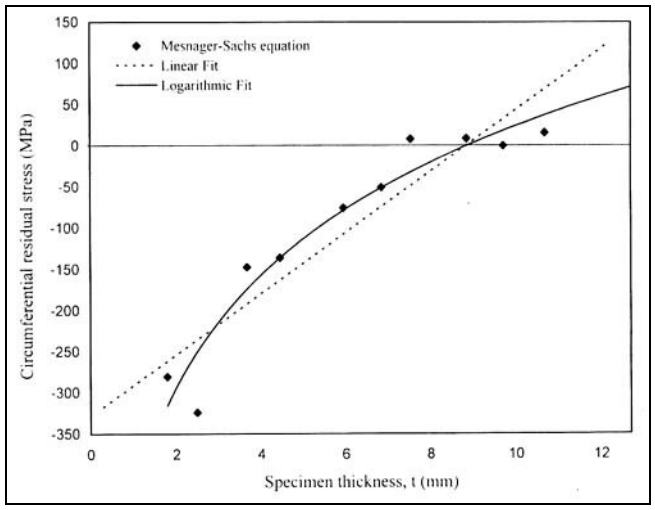

Figure 12: Circumferential residual stress distribution according to Mesnager-Sachs equation.

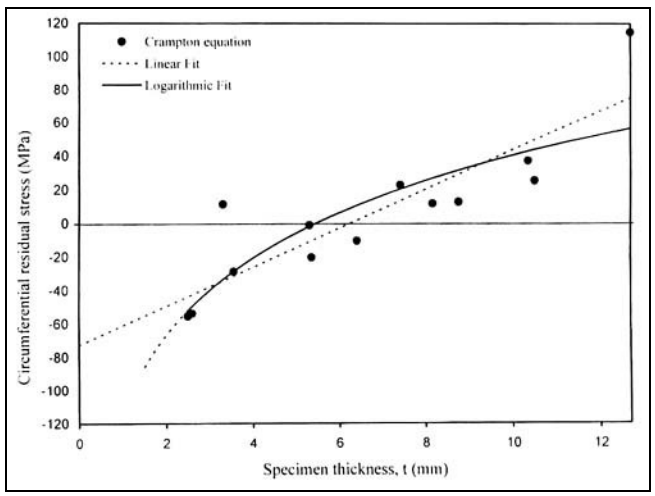

Figure 13: Circumferential residual stress distribution according to Crampton equation.

It is observed that the curves exhibited the same trend especially for V2 and V13. For a t=3.5 mm, ε_4 rose up to +550 μm/m and went down to -700 μm/m when the as-received fluctuated between +75 and -140 μm/m. A net difference was obtained when comparing zero relieved strain values.

3.3- Residual stress distribution

Using equations (2) and (7), circumferential residual stress distributions through wall thickness were obtained as illustrated respectively in figures 12 and 13. As tube thickness was reduced by layer removal from the inner side, the value of the residual stress decreased and changed sign from positive to negative. This finding confirmed that of displacements in figure 7. The calculated values presented some dispersion which was attributed to machining processes and to pipe inherent heterogeneity due to rolling. These results are comparable to those of literature [11-13,21-25] for piping and welding. The Mesnager-Sachs distribution (Fig. 12) was considered to be less effective since it does not account for the effect of longitudinal strains and gave high compressive stresses with a skewed distribution. Alternatively, the proposed equation by Crampton represented in a better way the distribution. This is obvious for the linear fit which generated an equilibrated distribution. Both data were subjected to logarithmic fits and the results are as follows:

Mesnager-Sachs equation:

$$\sigma_c = 206.13 Lnt - 482.66 \quad (10)$$

Crampton equation:

$$\sigma_c = 124.02 Lnt - 239.04 \quad (11)$$

The correlation coefficients were respectively 0.93 and 0.86. It is important to note that the zero value was approximately at 7.6 mm from the external diameter for the second case. The residual stresses at the pipe outer surface and at the bore were in the interval -156.3 MPa and +101.3 MPa that represented approximately 10 % of the material yield strength [20, 26]. These results may be used to study the effect of residual stress on reliability of underground pipes subjected to uniform corrosion and stress corrosion cracking phenomena.

CONCLUSION

The distribution of residual stresses through wall tube thickness was obtained by the layer removal method. It was found that compressive stresses acted on the outside layers of the pipe while tensile values dominated the bore side. The zero stress value was found at 7.6 mm depth using the Crampton equation, which exhibited a more realistic distribution, compared to Mesnager-Sachs model. This behavior is in good agreement with strain measurements during the cutting process. As the cutting notch was deepened, negative strain values are recorded passing by a zero value at 6.1 mm depth to become positive strains. The maximum residual stress value represented 10% of the material yield strength, a value that is fairly high to participate in damage due to stress corrosion cracking.

***Acknowledgments*:** We are grateful to ALFATUB Company for the furniture of the material and mechanical testing. We are also thankful to FERROVIAL Company for machining the large and heavy specimens. The financial support of SONATRACH National Oil Company, DP, Hassi Messaoud under Grant D-6001Z is greatly appreciated.

REFERENCES

[1]- Parkins R.N., Fesler R.R., "Line pipe stress corrosion cracking mechanisms and remedies", *Corrosion*, Paper N° 320 (1986).

[2]- Shahinian P., Judy R.W. Jr., "Stress corrosion crack growth in surface cracked panels of high strength steels", Stress corrosion - New approaches, ASTM, STP 610 (1976), pp.128-142.

[3]- Gray J.M., Pontremoly M., "Metallurgical options for grades X70 and X80 line pipe", International Conference on Pipe Technology, Rome, (1987), pp.171-191.

[4]- Shi P., Mahadevan S., "Corrosion fatigue and multiple site damage reliability analysis", *Int. J. Fatigue*, Vol. 25 (2003), pp.457-469.

[5]- Moulin D., Clement G., Drubay B., Goudet G., "Evaluation of ductile tearing in cracked pipes and elbows under bending", Nuclear Engineering and Design, Vol. 171 (2003), pp.33-43.

[6]- Orynyak I.V., Torop V.M., "Modelling of the limit state of thin-walled pipes with multiple axial coplanar defects", *Int. J. Pres. Ves. & Piping*, Vol. 70 (1996), pp.111-115.

[7]- Endos S. Nagae M., "Development of X100 UOE line pipe", The International Conference on Pipe Line Reliability, Calgary, 3 (1992), pp. 4.1-4.11.

[8]- Chattopadhyay J. Dutta, B.K., Kushwaha, H.S., Mahajan S.C., Kadodkar A., "Limit load analysis and safety assessment of an elbow with a circumferential crack under a bending moment", *Int. J. Pres. Ves. & Piping*, Vol. 62 (1995), pp.100-116.

[9]- Firmature R., Rahman S., "Elastic-plastic analysis of off-center cracks in cylindrical structures", *Engineering Fracture Mechanics*, Vol. 66 (2000), pp.15-39.

[10]- Michel B., Plancq D., "Lower bound limit load of a circumferentially cracked pipe under combined mechanical loading", *Nuclear Engineering and Design*, Vol. 185 (1998), pp.23-31.

[11]- Prevéy P.S., Cammett J.T., "The effect of shot-peening coverage on residual stress, cold work and fatigue in Ni-Cr-Mo low alloy steel", Proceedings of The International Conference on Shot-Peening, Sept. 16-20, Garmisch-Partenkirchen, Germany, (2002).

[12]- Prevéy P. Hornbach D. Mason P. Mahoney M., "Improving corrosion fatigue performance of AA2219 friction stir welds with low plasticity burnishing", International Surface Engineering Conference, Oct. 7-10, Columbus, OH. (2002).

[13]- Prevéy P., Hornbach D., Mason P., "Thermal residual stress relaxation and distortion in surface enhanced gas turbine engine components", Proceedings of the 17th Heat Treating Society Conference and Exposition, Eds. D.L. Milam et al., ASM, Materials Park, OH. (1998), pp.3-12.

[14]- Ahammed M., Melchers R.E., "Reliability estimation of pressurized pipelines subject to localized corrosion defects", *Int. J. Pres. Ves. & Piping*, Vol. 69 (1996), pp.267-272.

[15]- Kim Y.J, Schwalbe K.–H, Ainsworth R.A., "Simplified J-estimations based on the engineering treatment model for homogeneous and mismatched structures", *Engineering Fracture Mechanics,* Vol. 68 (2001), pp.9-27.

[16]- Zerbst U., Ainsworth R.A., Schwalbe K.-H., "Basic principles of analytical flaw assessment methods", *Int. J. Pres. Ves. & Piping*, Vol.77 (2000), pp.855-867.

[17]- Sachs G., "Internal stresses in metals", Zeitschrift des Vereines Deutcher Ingenieure, 71 (1927), pp.1511-1516.

[18]- Barrett C.S., "Internal stresses-A review", Metals and Alloys, 5 (1934), pp.131-154.

[19]- Lynch J.J., "The measurement of residual stresses", American Society for Metals, Residual Stress Measurements, Cleveland, OH. (1952), pp. 42-96.

[20]- Amirat A, Chaoui K., "Residual stress in seamless tubes", Synthèse, Revue des Sciences et Technologies de l'Université d'Annaba, (2001), pp.82-86.

[21]- Sorem Jr. J.R, Shadley J.R, Rybicki E.F., "Experimental method for determining through thickness residual hoop stresses in thin walled pipes and tubes without inside access", *Strain*, Vol. 26 (1990), pp.7-14.

[22]- Glinka G., "Residual stresses in fatigue and fracture: Theoretical analyses and experiments", in Residual stresses– generation, relaxation, measurement, prediction effects. A. Niku-Lari, Editor, Pergamon Press Ltd., UK (1986).

[23]- Ueda Y., Nakacho K., Shimizu T., "Improvement of residual stresses of circumferential joint of pipe by heat-sink welding", *Transactions of the ASME*, 108 (1986), pp.14-23.

[24]- ASTM STP 676, "Stress relaxation testing", Fox A., Editor, Philadelphia, PA., Committee E-28, (1979).

[25]- Harvey J.F., "Theory and Design of Pressure Vessels", Van Nostrand Reinhold Co. Inc., New York (1985).

[26]- Chaoui K., Amirat A., "Residual stress analysis in seamless X60 steel gas pipelines", 5ème Journées Scientifiques et Techniques, Hilton Hotel, Algiers, 16-18 December (2002)□